The Impact of Population III.1 Flash Reionization for Cosmic Microwave Background Polarization and Thomson Scattering Optical Depth

Citation for the original published paper (version of record):
Tan, J., Komatsu, E. (2026). The Impact of Population III.1 Flash Reionization for Cosmic Microwave Background Polarization
and Thomson Scattering Optical Depth. Astrophysical Journal Letters, 1005(1).
http://dx.doi.org/10.3847/2041-8213/ae7a6c

The Astrophysical Journal Letters, 1005:L32 (5pp), 2026 July 1 https://doi.org/10.3847/2041-8213/ae7a6c

The Impact of Population III.1 Flash Reionization for Cosmic Microwave Background Polarization and Thomson Scattering Optical Depth

Jonathan C. Tan[1,2] and Eiichiro Komatsu[3,4,5]
[1] Dept. of Physics & Astronomy, Chalmers University of Technology, Gothenburg, Sweden
[2] Dept. of Astronomy & Virginia Institute for Theoretical Astronomy, University of Virginia, Charlottesville, VA, USA
[3] Max-Planck-Institut für Astrophysik, Karl-Schwarzschild-Str. 1, 85741 Garching, Germany
[4] Ludwig-Maximilians-Universität München, Schellingstr. 4, 80799, München, Germany
[5] Kavli Institute for the Physics and Mathematics of the Universe (WPI), The University of Tokyo Institutes for Advanced Study (UTIAS), The University of Tokyo, Chiba 277-8583, Japan
Received 2026 April 10; revised 2026 May 31; accepted 2026 May 31; published 2026 June 26

Abstract

The Population III.1 theory for supermassive black hole (SMBH) formation predicts a very early ($z \sim 20$–25) transient phase, the "Pop III.1 Flash," of cosmic reionization powered by supermassive stars that are SMBH progenitors. The Universe then quickly recombines to become mostly neutral, with this state persisting until galaxies begin to reionize intergalactic gas again at $z \sim 10$. The overall Thomson scattering optical depth, τ, from the Flash has been shown to be $\tau_{\rm PopIII.1} \sim 0.03$, leading to a total $\tau \sim 0.08$–0.09. Such a value, while significantly larger than that previously inferred from Planck observations of the low-l EE polarization power spectrum of the cosmic microwave background (CMB), can help relieve several "tensions" faced by the standard ΛCDM cosmological model, especially the preference for negative neutrino masses and dynamic dark energy. Here we compute EE power spectra of example models of the Flash. We find that, because of its very high redshift, the contribution to $l \lesssim 6$ modes is dramatically reduced compared to usual low-z reionization models for the same value of τ, while the power at $l \gtrsim 6$ is boosted. Thus the Pop III.1 reionization scenario provides a natural way to increase τ, while remaining closer to the latest CMB low-l polarization observations.

Unified Astronomy Thesaurus concepts: Cosmology (343); Cosmic microwave background radiation (322); Galaxies (573)

1. Introduction

The epoch of cosmic reionization—the first billion years after the Big Bang—is a frontier of astrophysical and cosmological research today. Intense ultraviolet radiation from the first "Population III" stars, which were likely formed out of pristine hydrogen and helium gas in pregalactic dark matter halos, reionized the surrounding neutral atoms (see R. Barkana & A. Loeb 2001 for a review). However, we know very little about the time, process, and consequences of the formation of these first stellar sources.

The Population III.1 (hereafter Pop III.1) theory for supermassive black hole (SMBH) formation (N. Banik et al. 2019; J. Singh et al. 2023; V. Cammelli et al. 2025a) (see also J. C. Tan et al. 2024 for a review) proposes that SMBH-progenitor supermassive, i.e., $\sim 10^5\,M_\odot$, stars are born in "Pop III.1" minihalos, i.e., the first-forming, locally isolated, metal-free dark matter halos with masses $\sim 10^6\,M_\odot$ that are undisturbed by external feedback. These characteristics allow for the formation of a single massive star colocated with a highly concentrated dark matter cusp. Then the process of weakly interacting massive particle (WIMP) dark matter annihilation in the Pop III.1 protostar can affect its structure (D. Spolyar et al. 2008; A. Natarajan et al. 2009), in particular giving it a large photospheric radius with a relatively cool temperature (T. Rindler-Daller et al. 2015; D. Nandal et al. 2025; K. Topalakis et al. 2025). This allows the growing star to avoid early photoevaporative ionizing feedback that for "standard" Pop III stars, i.e., those not impacted by WIMP annihilation, typically truncates accretion around $100\,M_\odot$ during contraction to the zero-age main sequence (C. F. McKee & J. C. Tan 2008; J. C. Tan et al. 2010; T. Hosokawa et al. 2011; S. Hirano et al. 2014; H. Susa et al. 2014). Thus Pop III.1 protostars are theorized to be able to grow to $\sim 10^5\,M_\odot$, with this mass scale set by the baryonic content of the dark matter minihalo.

In the final stages of their evolution before they collapse to an SMBH, Pop III.1 supermassive stars are expected to become powerful sources of H-ionizing photons. These propagate quickly through the intergalactic medium (IGM), creating ionized regions (R-type H II regions), with typical radii of ∼1 comoving megaparsecs (cMpc). The feedback from these H II regions then sets the cosmic abundance of SMBHs, since Pop III.1 sources are required to have formed in pristine gas that was not impacted by a high level of ionization. In the fiducial case, the overall abundance of SMBHs is expected to be $n_{\rm SMBH} \sim 10^{-1}\,{\rm cMpc}^{-3}$ (J. C. Tan et al. 2024). The phase of Pop III.1 star formation ends by $z \sim 20$ (about 200 Myr after the Big Bang), after which the IGM quickly recombines. The gas only begins to be substantially ionized again once sufficient luminous galaxies have formed by $z \sim 10$ (about 500 Myr after the Big Bang).

The Pop III.1 theory thus predicts an early phase of ionization of the Universe, referred to as the "Pop III.1 Flash," in which a large fraction of the IGM at redshifts $z \sim 20$–25 was impacted. The contribution of the Pop III.1 Flash to the overall Thomson scattering optical depth of observed CMB photons has been evaluated to be $\tau_{\rm PopIII.1} \sim 0.03$ (J. C. Tan 2025).

This is a separate contribution from that associated with reionization of the Universe at lower redshifts ($z \lesssim 10$) by normal galaxies and active galactic nuclei (AGN) (B. E. Robertson et al. 2015; B. Greig & A. Mesinger 2017; J. B. Muñoz et al. 2024; M. Tang et al. 2024; Y. Kageura et al. 2025; A. Pahl et al. 2025; R. A. Meyer et al. 2025). The ionized IGM from this late-phase reionization is known to produce an optical depth of $\tau_{\rm gal} \simeq 0.06$. Such a level is consistent with previous results derived from the amplitude of the low-l *EE* modes of the CMB from the Planck Collaboration (Planck Collaboration et al. 2020), who found $\tau = 0.054 \pm 0.007$. Subsequent reanalyses of Planck data yielded slightly larger values, $\tau = 0.058 \pm 0.006$ (M. Tristram et al. 2024) and 0.0063 ± 0.005 (R. de Belsunce et al. 2021). Parametric reionization histories that are constrained by these CMB data indicate that this late-phase reionization began at $z \sim 10$ and ended at $z \sim 5$.

While the late-phase reionization by standard galaxies is consistent with the latest CMB results with $\tau \simeq 0.06$, a number of recent papers, which did not rely on the low-l polarization data, have argued for a larger value of $\tau \simeq 0.09$ (I. J. Allali et al. 2025, 2026; T. Jhaveri et al. 2025; N. Sailer et al. 2026). Such higher values would help alleviate tensions arising from CMB-based estimates of the Hubble constant (i.e., "Hubble tension") and from recent baryonic acoustic oscillation measurements from the Dark Energy Spectroscopic Instrument (DESI) (DESI Collaboration 2025), which, combined with Planck CMB results, manifest as a preference for negative neutrino masses (or positive, but too small, masses) and evolving, i.e., dynamic, dark energy. It has been pointed out by the above authors that the measurement of τ from the CMB faces a number of challenging systematic uncertainties, especially instrumental systematic effects (Planck Collaboration X 2014; Planck Collaboration VII 2016; Planck Collaboration Int. XLVI 2016), which might yet allow compatibility with a larger value. Nevertheless, as we discuss below, values of $\tau \simeq 0.09$ with standard late-phase reionization histories produce amplitudes of low-l *EE* modes that appear difficult to reconcile with Planck.

In this Letter we compute *EE* power spectra of example models of Pop III.1 reionization, i.e., with a very early phase of flash ionization, combined with standard late-phase contributions. We find that because of the very high redshift of the Pop III.1 ionization phase, the impact on the $l \lesssim 6$ CMB *EE* modes is dramatically reduced compared to the usual low-z *EE* contribution for the same value of τ, while the power at $l \gtrsim 6$ is boosted. We describe our methods in Section 2, give our results in Section 3, and discuss their implications in Section 4.

2. Methods

We parameterize the reionization history of the Universe with two components. For the late-phase, "low-z" component we adopt a standard $\tanh(z)$ function to describe the ionization fraction (defined as the ratio of the number density of free electrons to that of H nuclei) (A. Lewis 2008):

$$x_e(y) = \frac{f}{2}\left[1 + \tanh\left(\frac{y(z_{\rm re}) - y}{\Delta_y}\right)\right], \quad (1)$$

where $y(z_{\rm re}) = (1 + z_{\rm re})^{3/2}$ is the location where $x_e = f/2$, i.e., the "midway" point toward the maximum level of reionization, $\Delta_y = 1.5\sqrt{1 + z_{\rm re}}\Delta_z$, where Δ_z parameterizes the width of the transition, and, for the case of singly and doubly ionized He, $f = 1 + (n_{\rm He}/n_{\rm H}) \simeq 1.08$ and $1 + (2n_{\rm He}/n_{\rm H}) \simeq 1.16$, respectively. For low-$z$ reionization we adopt a standard treatment of He reionization: He is singly reionized when H is reionized and doubly reionized at $z = 3.5$ (A. Lewis 2008). We will also use the metric $x_{i,{\rm H}}$, which is the ionization fraction of H described by Equation (1) with $f = 1$.

For the high-z reionization associated with the Pop III.1 Flash, we follow the model of J. C. Tan (2025). This assumes supermassive Pop III.1 stars form at a redshift $z_{\rm form}$, leading to a subsequent peak level of ionization in their H II regions, $x_{i,{\rm H,peak}}$, at redshift $z_{\rm flash}$. These H II regions fill a significant volume fraction of the IGM, $f_{i,{\rm vol}}$. Following the results of the cosmological Pop III.1 SMBH seeding models (N. Banik et al. 2019; J. Singh et al. 2023), we consider two cases: $z_{\rm flash} = 20$ and 25. Note that these values are constrained by the requirement of forming sufficient SMBHs to match the observed population with $n_{\rm SMBH} \sim 10^{-2} - 10^{-1}\,{\rm cMpc}^{-3}$ (M. J. Hayes et al. 2024; V. Cammelli et al. 2025b).

For a fiducial case we consider values of $x_{i,{\rm H,peak}} = 1.0$ and $f_{i,{\rm vol}} = 0.5$, noting that there is a simple linear relationship between these parameters for the total contribution to τ. However, in the context of the Pop III.1 model, we require $f_{i,{\rm vol}}$ to be near unity. Similarly, H II regions undergoing *R*-type evolution are expected to have ionization fractions of order unity when the star is shining (M. Sanati et al. 2025). Our value of $x_{i,{\rm H,peak}}$ is a factor of 2 higher than that adopted by J. C. Tan (2025), which is motivated by our more accurate calculation of τ (see below).

The timescale for the ionization fraction to rise up to its peak value, $t_{\rm rise}$, is assumed to lie between the lifetime of the ionizing source and the time to establish a Strömgren sphere, $t_{\rm ion}$, in gas that has a density similar to that of the mean IGM density. For the former, we take a fiducial value of 10 Myr for the lifetime of a supermassive star that is somewhat prolonged by WIMP annihilation heating. For the latter, the value of $t_{\rm ion}$ assuming the mean cosmic density is

$$t_{\rm ion} = \frac{4}{3}\pi R_S^3 \frac{n_{\rm H}}{S} = \frac{1}{\alpha^{(2)} n_{\rm H}} \simeq 51.3\left(\frac{1 + z_{\rm form}}{31}\right)^{-3} {\rm Myr}, \quad (2)$$

where R_S is the radius of the Strömgren sphere, $n_{\rm H}$ is the total number density of H nuclei, $\alpha^{(2)} = 1.08 \times 10^{-13}(T/30{,}000\,{\rm K})^{-0.8}\,{\rm cm}^3\,{\rm s}^{-1}$ is the recombination rate to excited states of ionized H, where we have normalized to a fiducial temperature of $T = 30{,}000$ K expected in metal-free gas, and S is the rate of production of H-ionizing photons. The final calculation adopts the mean number density of H nuclei at $z = 30$, i.e., $n_{\rm H},\, z = 30 = 5.72 \times 10^{-3}\,{\rm cm}^{-3}$. For simplicity and given the uncertainty in Pop III.1 star ionizing spectra, we have ignored the reionization of He in this high-z reionization phase, although it is included in the low-z reionization component described by Equation (1).

Pop III.1 sources are expected to form in moderately overdense regions. For example, in the simulations of M. Sanati et al. (2025), the average density in the H II region around a Pop III.1 supermassive star is a factor of about 3 times greater than the cosmic average. From such simulations of ionizing feedback it is also seen that when $t_{\rm ion} > t_*$, the *R*-type ionization front continues to propagate

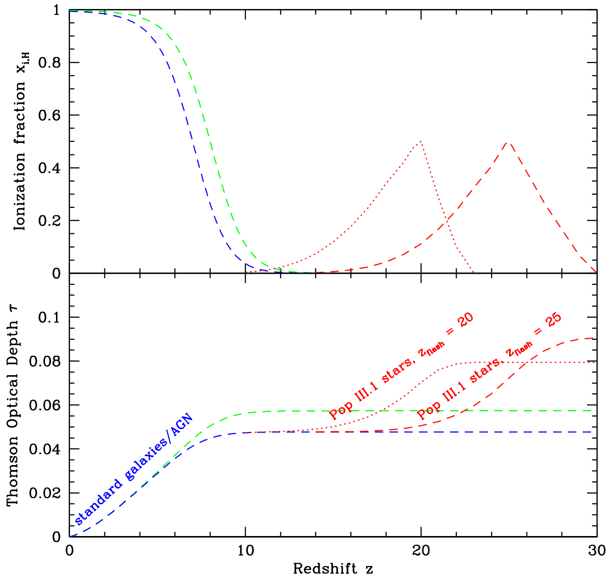

Figure 1. (a) Top: ionization fraction history of the Universe, shown as a function of redshift, with $x_{i,\mathrm{H}}$ measuring the fraction of H atoms that are ionized. The green dashed line shows a standard reionization history described with a tanh(z) function with $z_{\mathrm{re}} = 8$ (Equation (1)), from fully ionized conditions at low redshift to fully neutral conditions at high redshift. The dashed blue line is an equivalent model, but with $z_{\mathrm{re}} = 7$. Note, these models include a standard treatment of He reionization (see text). The red lines show fiducial ionization histories resulting from Pop III.1 supermassive stars, peaking at $z_{\mathrm{flash}} = 20$ (dotted) and 25 (dashed). (b) Bottom: Thomson optical depth to electron scattering, τ, integrated out to redshift, z. The green and blue dashed lines show the tanh(z) models with $z_{\mathrm{re}} = 8$ and 7, respectively, representing the contribution from "standard" galaxies and AGN. The red dotted and dashed lines show the contribution from Pop III.1 supermassive stars with epoch of peak flash ionization at $z_{\mathrm{flash}} = 20$ and 25, respectively, which have been combined with the tanh(z) with $z_{\mathrm{re}} = 7$ model.

after the star has ended its life. Given the above considerations, we adopt a fiducial value for $t_{\mathrm{rise}} = 30$ Myr. This implies that Pop III.1 stars would actually have started shining at $z_{\mathrm{form}} \simeq 23$ and 30 for our cases of $z_{\mathrm{flash}} = 20$ and 25, respectively. Thus t_{rise} can additionally be interpreted as encompassing a modest spread in formation redshifts of Pop III.1 stars that is similar in magnitude to these differences.

After reaching a peak ionization fraction in the Pop III.1 Flash, we assume that this level decreases exponentially on a timescale equal to the recombination timescale in the H II regions given by Equation (2), but adopting an overdensity compared to the mean IGM of a factor of 3. Note, given the R-type nature of the H II regions, there is limited impact on the density structure of the gas due to the ionizing feedback. For our cases of $z_{\mathrm{flash}} = 20$ and 25, these recombination times are 55 and 29 Myr, respectively.

We use a linear Boltzmann solver CLASS (D. Blas et al. 2011) to calculate the CMB *EE* power spectra for the various reionization histories, along with their associated values of τ. We assume a flat Lambda cold dark matter (ΛCDM) cosmological model with its parameters taken from "Plik best fit" in Table 1 of Planck Collaboration Int. LVII (2020): (h, $\Omega_c h^2$, $\Omega_b h^2$, $\ln(10^{10} A_s)$, n_s) = (0.6732, 0.12011, 0.022383, 3.0448, 0.96605), with the minimal total mass for neutrinos (0.06 eV). The total mass density parameter including the neutrino is $\Omega_m = 0.3158$, and the cosmological constant is given by $\Omega_\Lambda = 1 - \Omega_m$.

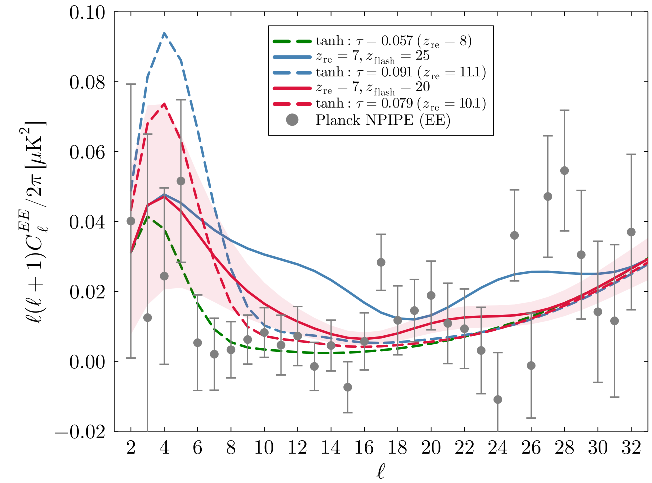

Figure 2. CMB *EE* power spectra for various reionization models. The green dashed line shows the tanh(z) model with $z_{\mathrm{re}} = 8$, yielding a total $\tau = 0.057$. The red and blue dashed lines show equivalent tanh(z) models with τ of 0.079 and 0.091, respectively. The red and blue solid lines show fiducial tanh(z) + Pop III.1 reionization models with $z_{\mathrm{flash}} = 20$ and 25 that also yield τ of 0.079 and 0.091, respectively. The shaded region around the red solid line shows a cosmic-variance-limited error range to the $z_{\mathrm{flash}} = 20$ model, assuming 70% sky coverage, i.e., a reasonable approximation for expected LiteBIRD uncertainties. The gray circles and error bars show the Planck NPIPE data (Planck Collaboration Int. LVII 2020; M. Tristram et al. 2021).

3. Results

Figure 1 shows some example reionization histories and associated cumulative distributions of $\tau(z) = c\sigma_T n_{\mathrm{H0}} \int_0^z dz\, x_e(z)(1+z)^2 H^{-1}(z)$, where c is the speed of light, σ_T the Thomson scattering cross section, n_{H0} the present-day number density of protons, and $H(z)$ the Hubble expansion rate. For the cases of late-phase reionization by "standard galaxies and AGN," these "tanh(z)" models are parameterized by z_{re} and $\Delta_z = 2$ (Equation (1)). The green and blue dashed lines show models with $z_{\mathrm{re}} = 8$ and 7, which yield total values of $\tau = 0.0573$ and 0.0477, respectively. To the latter model we also add on the high-z Flash component with $z_{\mathrm{flash}} = 20$ and 25 (both with $x_{i,\mathrm{H,peak}} = 1.0$ and $f_{i,\mathrm{vol}} = 0.5$), which yield total values of $\tau = 0.0794$ and 0.0906, respectively.

Figure 2 shows the low-l *EE* CMB power spectra from various reionization models compared to the Planck Public Release 4 (PR4) "NPIPE" data (Planck Collaboration Int. LVII 2020; M. Tristram et al. 2021). The green dashed line shows the tanh(z) model with $z_{\mathrm{re}} = 8$, which yields a good fit to the Planck data.

The red lines show models with τ elevated to 0.079. The dashed line shows the *EE* power spectrum when this τ is achieved via a standard tanh(z) function (requiring $z_{\mathrm{re}} = 10.1$). The solid line shows a model with tanh(z) with $z_{\mathrm{re}} = 7$ combined with a fiducial Pop III.1 contribution with $z_{\mathrm{flash}} = 20$. We find that even though these models have the same total value of τ, the amplitudes of the lowest l modes ($l \lesssim 6$) are significantly smaller for the model with the Pop III.1 component. Focusing on these $l \leqslant 6$ modes, i.e., those most commonly used to constrain cosmic reionization, then the Pop III.1 Flash model has $\chi^2 = 6.7$, while the tanh(z)-only model has $\chi^2 = 13.6$.

Similarly, the blue lines show two models with $\tau = 0.091$. The dashed line shows a case with a tanh(z) function (requiring $z_{\mathrm{re}} = 11.1$). The solid line shows the case with tanh(z) with $z_{\rm re} = 7$ combined with a fiducial Pop III.1 model with $z_{\rm flash} = 25$. The model with the Pop III.1 Flash component again has much lower power at $l \lesssim 6$. However we note that at intermediate scales with $7 \leqslant l \leqslant 18$ this model has significantly higher amplitudes that appear to be in tension with the latest Planck data.

This behavior can be explained as follows. CMB polarization is generated when an electron at a redshift of z scatters the quadrupole of the CMB as seen by the electron. The comoving wavenumber of the quadrupole as seen by the electron is given by $k \simeq 3/[r_L - r(z)]$, where $r_L = 14$ cGpc is the comoving distance from Earth to our last-scattering surface, and $r(z)$ is the comoving distance to redshift z. For example, a redshift of $z = 8$ yields $r(8) \simeq 9$ cGpc. We observe this wavenumber at a multipole of $l \leqslant kr(8) \simeq 6$, which corresponds to the so-called "reionization bump" in the polarization power spectra (M. Zaldarriaga 1997). As $r(z)$ increases with z, contributions to the EE power spectrum spread to larger values of l for sources at larger z. For a redshift of $z = 20$ relevant to the Pop III.1 Flash, we have $r(20) \simeq 11$ cGpc. Thus, $k \simeq 1$ cGpc^{-1} and the multipole is observed at $l \leqslant kr(20) \simeq 11$. We note that the secondary "peaks" at $l \sim 22$ and 26 for $z_{\rm flash} = 20$ and 25 are the result of an oscillation due to a spherical Bessel function of order 2.

4. Discussion and Conclusions

We have shown that reionization models including a component of Pop III.1 Flash ionization at redshifts of 20–25 yield CMB EE-mode power spectra with very different shapes compared to equivalent-τ standard late-phase reionization models described with a tanh(z) function (Equation (1)). In particular, if a certain elevated value of $\tau \simeq 0.08$–0.09 is desired, e.g., to alleviate tensions of "negative neutrino masses" or "dynamic dark energy" (I. J. Allali et al. 2025, 2026; T. Jhaveri et al. 2025; N. Sailer et al. 2026), then Pop III.1 models offer a way to do this that minimizes tension with the observed low-l CMB EE-mode constraints.

The sensitivity of the CMB EE power spectrum to the redshift dependence of reionization history has been discussed previously (e.g., M. Zaldarriaga et al. 2008; C. H. Heinrich et al. 2017; M. Millea & F. Bouchet 2018). However, the particular scenario of very early Pop III.1 Flash ionization has not been discussed in detail.

Future CMB polarization observations, e.g., with CLASS (Y. Li et al. 2025) and LiteBIRD (LiteBIRD Collaboration et al. 2023), are expected to be able to improve on the low-lE-mode constraints and thus test the proposed Pop III.1 reionization history. As we see from Figure 2, achieving an accuracy of ~20% in the range $10 \lesssim l \lesssim 30$ would be sufficient to distinguish different Pop III.1 models with $z_{\rm flash}$ in the range 20 to 25. LiteBIRD will deliver measurements of the EE power spectrum with a precision limited only by cosmic variance up to $l \simeq 200$. Such data will easily distinguish between the models shown in Figure 2.

Future studies of the CMB with the Simons Observatory (P. Ade et al. 2019) are expected to be able to further test the Pop III.1 prediction of an early phase of flash ionization, especially via observations of the patchy kinematic Sunyaev–Zel'dovich (pkSZ) effect from the peculiar motion of the H II regions. We note that current pkSZ constraints on reionization history, which have been found to be in 2σ tension with values of $\tau \simeq 0.09$ (C. Cain et al. 2025), have assumed a monotonically decreasing IGM ionization fraction with redshift. These need to be recalculated for the Pop III.1 scenario with a distinct phase of very early flash ionization. We also note that the peculiar motions driving the pkSZ signal are reduced at higher redshifts, so the Pop III.1 reionization scenario has an attractive feature of being able to boost τ in a way that minimizes additional pkSZ contributions. Furthermore, the fiducial Pop III.1 model predicts the formation of ionized bubbles with a typical size of 1 cMpc at $z \simeq 20$–25. These bubbles may leave an imprint on the pkSZ power spectrum (H. Park et al. 2013).

There are several other implications of the Pop III.1 model of early reionization, which have also been discussed by J. C. Tan (2025). These include signatures in high-z 21 cm emission that arise from ionized bubbles and/or heating effects on neutral gas around Pop III.1 sources. There is also a potential impact on the strength of the sky-averaged (global) 21 cm signal of neutral hydrogen absorption from the early Universe. A tentative detection of this signal, centered at $z = 17.2$, has been claimed based on analysis of data from the low-band antenna of the Experiment to Detect the Global EoR Signature (EDGES) (J. D. Bowman et al. 2018) (however, see S. Singh et al. 2022). However, the absorption depth seen is at least twice as strong as predicted by standard astrophysical scenarios in ΛCDM. A potential resolution of this anomalous absorption is an enhanced radio background, equivalent to a brightness temperature of 67.2 K, significantly greater than that of the CMB at these redshifts with $T_{\rm CMB} = 49.5$ K (e.g., C. Feng & G. Holder 2018; A. Fialkov & R. Barkana 2019). J. C. Tan (2025) has presented a simple estimate of the expected free–free emission from the Flash, finding that for reasonable choices of parameters, it is able to produce a radio background strong enough to explain the deep absorption depth of the EDGES result.

Finally, the most fundamental implication of the Pop III.1 cosmological model for SMBH formation is that it requires energy input from self-annihilating dark matter in the very first generation of stars. In the framework of ΛCDM cosmology, the most natural way for this to occur is via capture and decay of WIMPs in primordial protostars (D. Spolyar et al. 2008; A. Natarajan et al. 2009; T. Rindler-Daller et al. 2015; D. Nandal et al. 2025; K. Topalakis et al. 2025), with particle masses of $m_\chi \sim 100$–1000 GeV and self-annihilation rate coefficients of $\langle\sigma_a v\rangle \simeq 3 \times 10^{-26}\,{\rm cm^3\,s^{-1}}$ (e.g., G. Jungman et al. 1996) to explain the cosmic dark matter density, $\Omega_{\rm DM} = 0.268$. Thus a basic prediction of the Pop III.1 model (and more generally of such ΛCDM models) is the existence of WIMPs with the above properties, with implications for direct and indirect dark matter search experiments. In this context, the recent claim (T. Totani 2025) of a ~20 GeV gamma-ray excess seen in Fermi Large Area Telescope (LAT) data in the halo region of the Milky Way, which implies a WIMP mass of ~500 GeV, is intriguing and warrants further investigation.

Acknowledgments

We thank Richard Ellis for helpful discussions and Matthieu Tristram for his help with the Planck NPIPE data. We also thank "Giesinger Bräu Stehausschank" for their hospitality, where the original idea for this project emerged. We thank Robert Lupton and his collaborators for developing the SuperMongo graphics software and Ned Wright for developing his Java Script Cosmology Calculator (E. L. Wright 2006). J.C.T. acknowledges funding from the Chalmers Initiative on Cosmic Origins (CICO), the Virginia Initiative on Cosmic Origins (VICO), and the Virginia Institute for Theoretical Astrophysics (VITA), supported by the College and Graduate School of Arts and Sciences at the University of Virginia. E.K.'s work was supported in part by the Excellence Cluster ORIGINS, which is funded by the Deutsche Forschungsgemeinschaft (DFG, German Research Foundation) under Germany's Excellence Strategy: grant No. EXC-2094–390783311. The Kavli IPMU is supported by World Premier International Research Center Initiative (WPI), MEXT, Japan.

ORCID iDs

Jonathan C. Tan https://orcid.org/0000-0002-3389-9142
Eiichiro Komatsu https://orcid.org/0000-0002-0136-2404

References

Ade, P., Aguirre, J., Ahmed, Z., et al. 2019, JCAP, 2019, 056
Allali, I. J., Li, L., Singh, P., & Fan, J. 2026, PhRvD, 113, 083515
Allali, I. J., Singh, P., Fan, J., & Li, L. 2025, JCAP, 2025, 082
Banik, N., Tan, J. C., & Monaco, P. 2019, MNRAS, 483, 3592
Barkana, R., & Loeb, A. 2001, PhR, 349, 125
Blas, D., Lesgourgues, J., & Tram, T. 2011, JCAP, 07, 034
Bowman, J. D., Rogers, A. E. E., Monsalve, R. A., Mozdzen, T. J., & Mahesh, N. 2018, Natur, 555, 67
Cain, C., Van Engelen, A., Croker, K. S., et al. 2025, ApJL, 987, L29
Cammelli, V., Monaco, P., Tan, J. C., et al. 2025a, MNRAS, 536, 851
Cammelli, V., Tan, J. C., Young, A. R., et al. 2025b, ApJ, 991, 141
de Belsunce, R., Gratton, S., Coulton, W., & Efstathiou, G. 2021, MNRAS, 507, 1072
DESI Collaboration 2025, PhRvD, 112, 083515
Feng, C., & Holder, G. 2018, ApJL, 858, L17
Fialkov, A., & Barkana, R. 2019, MNRAS, 486, 1763
Greig, B., & Mesinger, A. 2017, MNRAS, 465, 4838
Hayes, M. J., Tan, J. C., Ellis, R. S., et al. 2024, ApJL, 971, L16
Heinrich, C. H., Miranda, V., & Hu, W. 2017, PhRvD, 95, 023513
Hirano, S., Hosokawa, T., Yoshida, N., et al. 2014, ApJ, 781, 60
Hosokawa, T., Omukai, K., Yoshida, N., & Yorke, H. W. 2011, Sci, 334, 1250
Jhaveri, T., Karwal, T., & Hu, W. 2025, PhRvD, 112, 043541
Jungman, G., Kamionkowski, M., & Griest, K. 1996, PhR, 267, 195
Kageura, Y., Ouchi, M., Nakane, M., et al. 2025, ApJS, 278, 33
Lewis, A. 2008, PhRvD, 78, 023002
Li, Y., Eimer, J. R., Appel, J. W., et al. 2025, ApJ, 986, 111
LiteBIRD Collaboration, Allys, E., Arnold, K., et al. 2023, PTEP, 2023, 042F01
McKee, C. F., & Tan, J. C. 2008, ApJ, 681, 771
Meyer, R. A., Roberts-Borsani, G., Oesch, P. A., & Ellis, R. S. 2025, MNRAS, 542, 1952
Millea, M., & Bouchet, F. 2018, A&A, 617, A96
Muñoz, J. B., Mirocha, J., Chisholm, J., Furlanetto, S. R., & Mason, C. 2024, MNRAS, 535, L37
Nandal, D., Topalakis, K., Tan, J. C., et al. 2025, arXiv:2507.00870
Natarajan, A., Tan, J. C., & O'Shea, B. W. 2009, ApJ, 692, 574
Pahl, A., Topping, M. W., Shapley, A., et al. 2025, ApJ, 981, 134
Park, H., Shapiro, P. R., Komatsu, E., et al. 2013, ApJ, 769, 93
Planck Collaboration, Aghanim, N., Akrami, Y., et al. 2020, A&A, 641, A6
Planck Collaboration Int. LVII 2020, A&A, 643, A42
Planck Collaboration Int. XLVI 2016, A&A, 596, A107
Planck Collaboration VII 2016, A&A, 594, A7
Planck Collaboration X 2014, A&A, 571, A10
Rindler-Daller, T., Montgomery, M. H., Freese, K., Winget, D. E., & Paxton, B. 2015, ApJ, 799, 210
Robertson, B. E., Ellis, R. S., Furlanetto, S. R., & Dunlop, J. S. 2015, ApJL, 802, L19
Sailer, N., Farren, G. S., Ferraro, S., & White, M. 2026, PhRvL, 136, 081002
Sanati, M., Tan, J. C., Devriendt, J., et al. 2025, MNRAS, 542, 1532
Singh, J., Monaco, P., & Tan, J. C. 2023, MNRAS, 525, 969
Singh, S., Jishnu, N. T., Subrahmanyan, R., et al. 2022, NatAs, 6, 607
Spolyar, D., Freese, K., & Gondolo, P. 2008, PhRvL, 100, 051101
Susa, H., Hasegawa, K., & Tominaga, N. 2014, ApJ, 792, 32
Tan, J. C. 2025, ApJL, 989, L47
Tan, J. C., Singh, J., Cammelli, V., et al. 2024, arXiv:2412.01828
Tan, J. C., Smith, B. D., & O'Shea, B. W. 2010, AIPC, 1294, 34
Tang, M., Stark, D. P., Topping, M. W., Mason, C., & Ellis, R. S. 2024, ApJ, 975, 208
Topalakis, K., Nandal, D., & Tan, J. C. 2025, arXiv:2510.00216
Totani, T. 2025, JCAP, 2025, 080
Tristram, M., et al. 2021, A&A, 647, A128
Tristram, M., et al. 2024, A&A, 682, A37
Wright, E. L. 2006, PASP, 118, 1711
Zaldarriaga, M. 1997, PhRvD, 55, 1822
Zaldarriaga, M., Colombo, L., Komatsu, E., et al. 2008, arXiv:0811.3918